Neural correlates of dynamic adaptation and motor memory formation in two-degree of freedom wrist pointing

Andria J. Farrens,[1] and Fabrizio Sergi[1]

***Abstract*— We developed a novel fMRI-compatible wrist robot, the MR-SoftWrist, to study the neural processes that underlie dynamic adaptation. Here we present our first study on thirty-four healthy young adults. Our results validate the MR-SoftWrist as a tool for investigating dynamic adaptation of the wrist during fMRI, and establish the behavioral characteristics and neural activations associated with active motor control and off-line neural processing of dynamic adaptation.**

I. INTRODUCTION

Adaptation is a common framework used to study motor learning in the laboratory setting [1]. Adaptation refers to the error-driven process of adjusting ones motor actions to changes in task dynamics. Following adaptation, behavioral evidence suggests that adapted motor plans are consolidated into motor memories that contribute to faster relearning on re-exposure to the same dynamic condition.

Adaptation has been studied using visuomotor distortions in 2-degree of freedom (DOF) wrist pointing tasks, and using dynamic perturbations in whole arm reaching tasks, but not in the context of dynamic perturbations in 2-DOF wrist pointing. Moreover, due to restrictions imposed by fMRI compatibility, few previous studies have investigated the neural correlates of dynamic adaptation, and those that did used large-movement amplitude tasks that can cause confounds in the fMRI data [2].

To use fMRI to measure the neural correlates of dynamic adaptation, our group has developed an fMRI-compatible robot, the MR-SoftWrist, to apply dynamic perturbations during low-movement amplitude wrist pointing tasks. Here, we present the results of our first fMRI study on thirty-four healthy young adults. Our results establish the behavioral characteristics of dynamic adaptation of the wrist to a 2-DOF curl-force field, and the neural correlates of active dynamic adaptation and the ensuing off-line changes associated with motor memory formation.

II. METHODS

A. MR-SoftWrist

The MR-SoftWrist (Fig. 1, top left) supports wrist flexion-extension (FE) and radial-ulnar deviation (RUD) in a circular workspace with a radius of 20 deg. The MR-SoftWrist has a maximum output torque of 1.5 N·m, and measures end-effector force, velocity and position at a rate of 1000 Hz. For an in-depth description of its design and control see [3], and for its fMRI compatibility see [4].

*Work supported by the AHA Scientist Development Grant 17SDG33690002, by the University of Delaware Research Foundation grant no. 16A01402, by the ACCEL NIGMS IDeA grant U54-GM104941.

[1] Human Robotics Lab, Department of Biomedical Engineering, University of Delaware, Newark, DE USA. afarrens@udel.edu, zonni@udel.edu, fabs@udel.edu

B. Experimental protocol

Our protocol included three motor tasks interleaved with three resting state scans (Fig. 1). Motor tasks were used to assess neural activity associated with task performance, while resting state scans were used to assess off-line changes in functional activity associated with motor memory formation [5]. For all motor tasks, participants held the handle of the MR-SoftWrist with their dominant (right) hand to control a cursor displayed on a screen that was visible during fMRI. FE of the wrist moved the cursor horizontally, while RUD moved the cursor vertically; radio-ulnar rotations were prevented by a forearm support. Participants were cued to make alternating FE rotations to move the cursor in a straight path between two targets placed at (± 10 FE, 0 RUD) deg.

The first motor task was a no force (NF) task, in which the robot acted transparently to measure motor performance with minimal interaction forces. The second task was a curl-force (CF) task, in which the robot applied a velocity-dependent torque, $[\tau_{FE}, \tau_{RUD}] = B[\dot{\theta}_{FE}, \dot{\theta}_{RUD}]$, $B = [0, 2.5; -2.5, 0]$ mN·m·s/rad, to apply perturbations lateral to the direction of movement. The final task was a velocity dependent resistive force (RF) task, with $\tau = B\dot{\theta}$, $B = [-2.5, 0; 0, -2.5]$ mN·m·s/rad, such that impedance increased in the direction of movement. In all tasks, error-clamp trials were placed with a $1/8^{th}$ frequency to sample subject generated forces without disrupting adaptation [**?**]. All tasks had blocks of 24 trials with 15 sec. breaks between blocks. FMRI data, with 2 mm^3 resolution and 1 sec. TR, were collected via a 64-channel head coil on a 3T Siemens scanner.

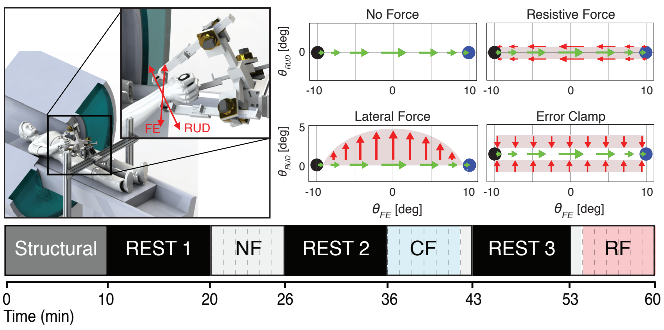

Fig. 1. Top left: MR-SoftWrist in its operating condition. Top right: Task-specific force conditions; robot applied force is shown in red, cursor velocity in green. Bottom: fMRI task design. Rest conditions were 10 minutes each. For each motor task, blocks are demarked by dashed lines; no force blocks are shown in grey, curl force in blue, and resistive force in pink.

C. Data Analysis

1) Behavioral: Motor performance was quantified via trajectory error (TE), defined as the internal angle between the maximal deviation of the cursor and the start and end targets within the first 150 ms of trial onset (counter-clockwise positive). Change in force production, termed adaptation index (AI), was quantified as β_1 from the regression of the measured force profile in EC trials onto the ideal compensatory curl-force profile: $F_{actual}(t) = \beta_1 F_{ideal}(t) + \beta_0(t) + \varepsilon(t)$ [1]. We used one-way repeated measures ANOVAs to assess the effect of task (NF, CF, RF) on TE and AI in each block.

2) fMRI data: All fMRI data were realigned and normalized into standard (MNI) space. We used a blocked general linear model to investigate the effect of each task (NF, CF, RF) compared to rest, with head motion included as nuisance regressors. To identify neural activity associated with dynamic adaptation, we preformed a group-level contrast between the CF-rest and NF-rest subject-level beta-maps. A group level contrast between CF-rest and RF-rest was used to control for neural activity associated with force.

We restricted our main resting state functional connectivity (rsFC) analysis to regions within the cortico-thalamic-cerebellar (CTC) network, previously associated with motor adaptation (Fig. 2, C) [1], [2], and performed an exploratory analysis of rsFC between all anatomical regions with significant curl force task related activation. Functional connectivity was defined as the correlation of the average signal measured in one brain region to another. Comparison of rsFC measured in Rest 1 to Rest 3 was used to assess change associated with off-line processing of dynamic adaptation. Comparison of rsFC in Rest 1 to Rest 2 was used as a control for changes in rsFC assocaited with motor performance.

III. RESULTS

A. Behavioral Metrics

The one-way ANOVA showed a significant effect of task on TE and AI ($p < 0.001$). Post-hoc analysis of TE showed characteristic effects of adaptation, including a significant increase in initial errors in the CF task that significantly decreased across the CF task, as well as signifcant after effects (Fig. 2, A). Post-hoc analysis of AI showed significant increases in AI in the CF task, indicative of adaptation. The final magnitude of AI achieve in our study (0.34 ± 0.1) was lower than is typically reported in the literature (>0.5) [1]. This difference may be due to the concurrent use of co-contraction strategies to reject dynamic perturbations, or an artifact of the MR-SoftWrist's measurement capabilities.

B. fMRI Analysis

In all tasks, activations were predominantly localized in the left motor cortex, left thalamus and right cerebellum, in line with current knowledge on motor control. Activation in the posterior parietal cortex, which is associated with predictive planning of spatial and temporal aspects of movement, was significant only in the CF task [1]. The contrast between CF and NF tasks showed significantly greater activation in the right sensorimotor areas and left anterior cerebellum (Fig. 2, B), that remained significant in the CF versus RF task contrast. As such, curl-force adaptation may require greater recruitment of non-dominant cortico-cerebellar pathways.

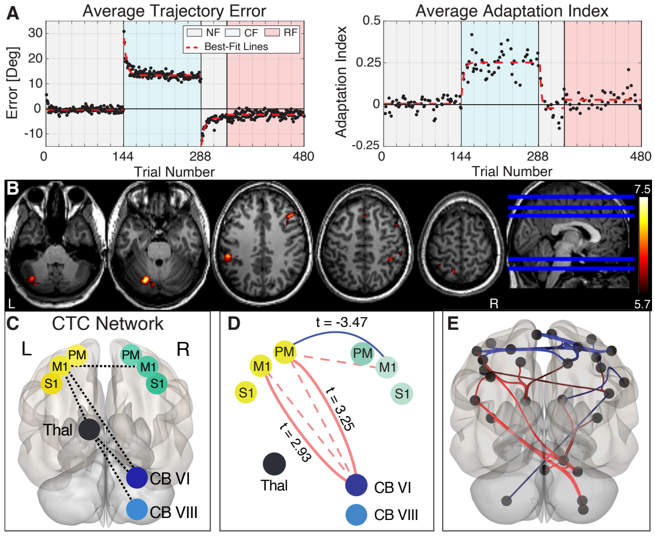

Fig. 2. A) Group average behavior measured across all motor tasks. B) Axial slices of CF−rest > NF−rest group contrast ($P_{FWE} < 0.05$). C) Main rsFC analysis brain regions, and D) Rest 3-Rest 1 results. Dashed lines: baseline rsFC; Curved lines: change in rsFC; Red: positive/increased rsFC; Blue: decreased rsFC. E) Results of supplementary rsFC analysis, Rest 3-Rest 1 ($T > 3$, $P_{NBS,FDR} < 0.05$). Black spheres denote brain regions with significant change, red lines: increased rsFC, blue lines: decreased rsFC.

In both rsFC analyses, comparison of Rest 3 to Rest 1 showed significant increases in rsFC between the left cortical motor areas and the right cerebellum, as well as a decrease in interhemispheric rsFC between the motor cortices (Fig. 2, D-E). No significant change was measured between Rest 2 and Rest 1. These results suggest that the trained CTC network is engaged in motor memory formation that is independent from the untrained right cortical motor areas.

IV. CONCLUSIONS

Our behavioral results confirm that adaptation occurs in response to curl-force perturbations applied during 2-DOF wrist pointing, and our fMRI analysis established neural activaitions and changes in rsFC that are unique to adaptation. Future work will include validating our behavioral results with another wrist robot, and investigating the relationship between rsFC and behavioral measures of adaptation.

REFERENCES

[1] Reza Shadmehr, Maurice A Smith, and John W Krakauer. Error Correction, Sensory Prediction, and Adaptation in Motor Control. *Annu. Rev. Neurosci*, 33:89–108, 2010.

[2] J. Diedrichsen. Neural Correlates of Reach Errors. *Journal of Neuroscience*, 25(43):9919–9931, 2005.

[3] Andrew Erwin, Marcia K O Malley, David Ress, and Fabrizio Sergi. Development , Control , and MRI-Compatibility of the MR-SoftWrist. *IEEE ICORR*, pages pp. 187–192, 2015.

[4] A. J. Farrens and et. al. Quantitative Testing of fMRI-compatibility of an Electrically Active Mechatronic Device for Robot-Assisted Sensorimotor Protocols. *IEEE Trans. on Biomed Eng*, pages 1–13, 2017.

[5] B Biswal, Yetkin FZ, Haughton VM, and Hyde JS. Functional connectivity in the motor cortex of resting human brain using. *Magn Reson Med*, 34(9):537–541, 1995.